JACS
JOURNAL OF THE AMERICAN CHEMICAL SOCIETY

ARTICLE

pubs.acs.org/JACS

Room Temperature Water Splitting at the Surface of Magnetite

Gareth S. Parkinson,* Zbyněk Novotný, Peter Jacobson, Michael Schmid, and Ulrike Diebold*

Institute of Applied Physics, Vienna University of Technology, Vienna, Austria

ABSTRACT: An array of surface science measurements has revealed novel water adsorption behavior at the $Fe_3O_4(001)$ surface. Following room temperature exposure to water, a low coverage of hydrogen atoms is observed, with no associated water hydroxyl group. Mild annealing of the hydrogenated surface leads to desorption of water via abstraction of surface oxygen atoms, leading to a reduction of the surface. These results point to an irreversible splitting of the water molecule. The observed phenomena are discussed in the context of recent DFT calculations (Mulakaluri, N.; Pentcheva, R.; Scheffler, M. *J. Phys. Chem. C* **2010**, *114*, 11148), which show that the Jahn−Teller distorted surface isolates adsorbed H in a geometry that could kinetically hinder recombinative desorption. In contrast, the adsorption geometry facilitates interaction between water hydroxyl species, which are concluded to leave the surface following a reactive desorption process, possibly via the creation of O_2.

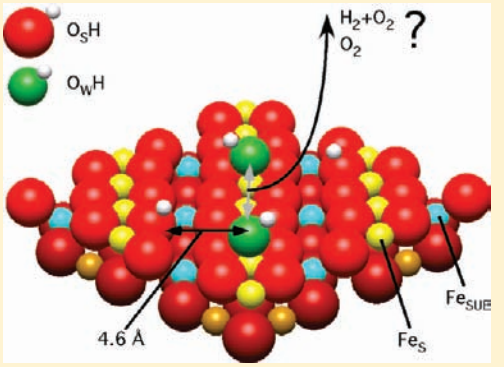

1. INTRODUCTION

The ubiquity of both water and oxide surfaces in the environment ensures that their interactions represent some of the most fundamental chemical reactions occurring in nature. Moreover, water−oxide interactions underpin many areas of science and technology including heterogeneous catalysis, electrochemistry, corrosion processes, and environmental science. Until recently, utilization of the surface science approach to understanding such interactions at the atomic scale, which has yielded tremendous insight for water−metal interactions,[1−5] has been precluded for many oxides by a lack of basic knowledge about the surface structure. However, where this knowledge is in place, for example, for $TiO_2(110)$[6−8] and $ZnO(10\bar{1}0)$,[9−14] water adsorption has been demonstrated to be both molecular and dissociative, with the surface termination and defects such as O vacancies (V_O) playing a significant role. In the presence of V_O, it is thought that water adsorbs dissociatively according to eq 1,[6−14] with the water hydroxyl (O_WH) filling the vacancy to create a surface hydroxyl (O_SH), and the dissociated H atom forming a second O_SH with a nearby surface oxygen atom (O_S),

$$H_2O_W + V_O + O_S \rightarrow O_SH + O_SH \quad (1)$$

Dissociative adsorption in the absence of V_O results in an adsorbed surface hydroxyl (O_WH) containing the oxygen atom from the water and an O_SH, according to eq 2,

$$H_2O_W + O_S \rightarrow O_WH + O_SH \quad (2)$$

In this article, we report the remarkable observation that water exposure to the nondefective, stoichiometric $Fe_3O_4(001)$ surface at room temperature (RT) results only in the adsorption of a low coverage of O_SH, that is, H adsorbed on the oxygen sublattice. Heating this hydrogenated surface to 520 K leads to desorption of water through the abstraction of lattice O_S atoms (Mars − van Krevelen mechanism). Thus, exposure to water vapor reduces the $Fe_3O_4(001)$ surface under our experimental conditions. We argue that this hitherto unreported adsorption behavior for water occurs because recombinative desorption of water is kinetically hindered by the adsorption geometry. Consequently, alternative reactions between O_WH can occur, leading to desorption at room temperature, possibly as H_2 and O_2.

2. EXPERIMENTAL DETAILS

The experiments described here were performed in two separate ultra high vacuum (UHV) systems. The first system comprises separate vessels for preparation (base pressure = 1×10^{-10} mbar) and analysis (base pressure = 5×10^{-11} mbar), with capability for low energy electron diffraction (LEED), X-ray photoelectron spectroscopy (XPS), and scanning tunneling microscopy (STM). The low energy ion scattering (LEIS) measurements were performed in a UHV chamber also equipped for LEED and Auger electron spectroscopy (AES) analysis. The measurements were performed using a synthetic Fe_3O_4 single crystal that was grown using the floating zone method by Z. Mao and co-workers at Tulane University, New Orleans, LA. The crystal was oriented, cut, and polished by Mateck GmbH. The clean stoichiometric $Fe_3O_4(001)$ surface was prepared using sputter and anneal cycles. The cycles comprise sputtering with 1 keV Ar^+ ions (sample current 1.5 μA) and subsequent annealing at ~1000 K for 1 h in 2×10^{-6} mbar O_2. A sharp $(\sqrt{2} \times \sqrt{2})R45°$ LEED pattern was observed (not shown) and no contamination was detectable in XPS survey spectra. Deionized H_2O was further purified using freeze−pump−thaw cycles and was dosed into either the preparation or analysis vessel of the STM system through high precision leak valves. Isotopically labeled $H_2{}^{18}O$ (Sigma-Aldrich) was purified using a similar freeze−pump−thaw procedure and was dosed directly into the LEIS system also using a high precision leak valve.

Received: April 14, 2011
Published: July 08, 2011

STM measurements were carried out using a SPECS Aarhus 150 STM with electrochemically etched W tips. All STM images were taken in the constant-current mode imaging empty states (V_{sample} = +0.7 to +1.8 V and I_{tunnel} from 0.15 to 0.3 nA) at RT. The time between the water dosing and the onset of the STM measurements was typically ca. 15 min. Images acquired thereafter showed no dependence on time with indistinguishable appearance over several hours.

To check that typical components of the residual gas in our UHV chamber do not influence the sample surface, we have independently dosed 100 Langmuir CO, H_2, and O_2 to the sample surface at room temperature and observed STM images representative only of the clean $Fe_3O_4(001)$ surface. Similarly, XPS spectra show no contamination of the surface with C in our detection limit following CO dosing, and following the water dosing experiments described here.

3. RESULTS

3.1. Scanning Tunneling Microscopy Studies: Adsorption.

A schematic model of the energetically favorable $Fe_3O_4(001)$ surface, as determined by a density functional theory (DFT) and quantitative low energy electron diffraction (LEED-IV) investigation,[15,16] is shown in Figure 1a. The surface adopts a $(\sqrt{2} \times \sqrt{2})R45°$ superstructure following a Jahn−Teller distortion, doubling the periodicity along the [110] direction. This structural model corresponds well with STM images,[17−19] in which undulating anti-phase rows attributable to surface Fe atoms (Fe_S) are observed (see Figure 1b). The symmetry reduction results in an inequivalence between the two surface O sites without a subsurface Fe (Fe_{SUB}) neighbor; in the bulk, these two O sites are identical. Oxygen atom $O_{NAR.}$ is located where the Fe_S rows are relaxed together and O_{WIDE} is located where the undulations render the Fe_S rows further apart.

Exposure of the clean surface to 22.5 Langmuir (L, 1 L = 1.33×10^{-6} mbar·s) water vapor at RT results in the appearance of several bright double protrusions located over Fe_S sites (Figure 1c). Identical protrusions were observed as a result of atomic H deposition in a previous study,[20] and consequently, we attribute them to O_SH species (white atom in the model in Figure 1c). STM does not directly image the O_SH, but their presence leads to a modification of the density of states (DOS) in the neighboring Fe_S atom pair (colored orange in the model in Figure 1c), enhancing their contrast in STM images.[20] Adsorbed H atoms relax toward the symmetrically equivalent $O_{NAR.}$ atom from the atop site within the surface unit cell, forming a hydrogen bond.[20] It is important to note that diffusion of this adsorbed H at room temperature occurs only between the two symmetrically equivalent $O_{NAR.}$ atoms, as indicated by the dashed black arrows in Figure 1a.

In Figure 2, we show a series of STM images acquired following exposure of the clean $Fe_3O_4(001)$ surface to water at room temperature, with nominal exposures ranging from 0.045 to 90 L. For the lowest exposures (0.045 and 0.45 L), 0.01 ML O_SH is observed (here 1 ML O_SH is defined relative to the number of O_S atoms, and is comparable to the saturation coverage achieved through the deposition of atomic H[20]). The O_SH are not randomly distributed, but appear as pairs in neighboring unit cells; two such paired O_SH are marked in Figure 2 with yellow half circles. Consistent with prior work, we expect the vacancy to be filled by the O_WH, with the extra H bound to a nearby O site. Consequently, paired O_SH are compatible with the reaction of water with V_O as described by eq 1. Increasing the water exposure by another order of magnitude (to 4.5 L) leads to an increased coverage of 0.013 ML. The surface still exhibits 0.01 ML paired O_SH, with the difference made up by several *isolated* O_SH species. This suggests that the increase in H coverage above 0.01 ML is not due to the reaction of water with V_O as described by eq 1 but that the additional O_SH species stem from dissociative adsorption at regular lattice sites (eq 2). One would then expect O_WH in addition to O_sH, but interestingly, no feature is observed that could be attributed to such a species. Further increasing the water exposure to 22.5 L leads to an increased O_SH coverage (0.044 ML). The majority

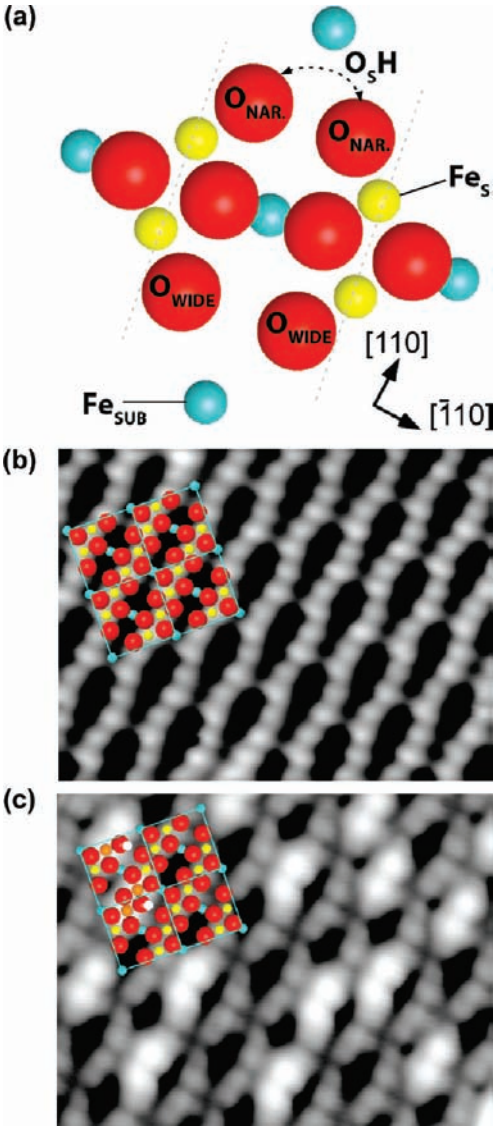

Figure 1. (a) Schematic model of the Jahn−Teller distorted $Fe_3O_4(001)$ surface unit cell. Two inequivalent O_S sites labeled $O_{NAR.}$ and O_{WIDE} are located where the neighboring Fe_S rows are closer together and wider apart, respectively. H adsorbs at $O_{NAR.}$ sites and can diffuse between neighboring $O_{NAR.}$ atoms as indicated by the dashed arrow. (b) High resolution STM image (5×3.5 nm^2, V_{sample} = +1 V, I_{tunnel} = 0.3 nA) of the clean $Fe_3O_4(001)$ surface with a superimposed structural model comprising four surface unit cells. (c) High resolution STM image (5×3.5 nm^2, V_{sample} = +1 V, I_{tunnel} = 0.3 nA) of the $Fe_3O_4(001)$ surface following exposure to 22.5 Langmuir water vapor at room temperature. The pairs of bright protrusions stem from H atoms adsorbed at $O_{NAR.}$

dx.doi.org/10.1021/ja203432e |*J. Am. Chem. Soc.* 2011, 133, 12650–12655

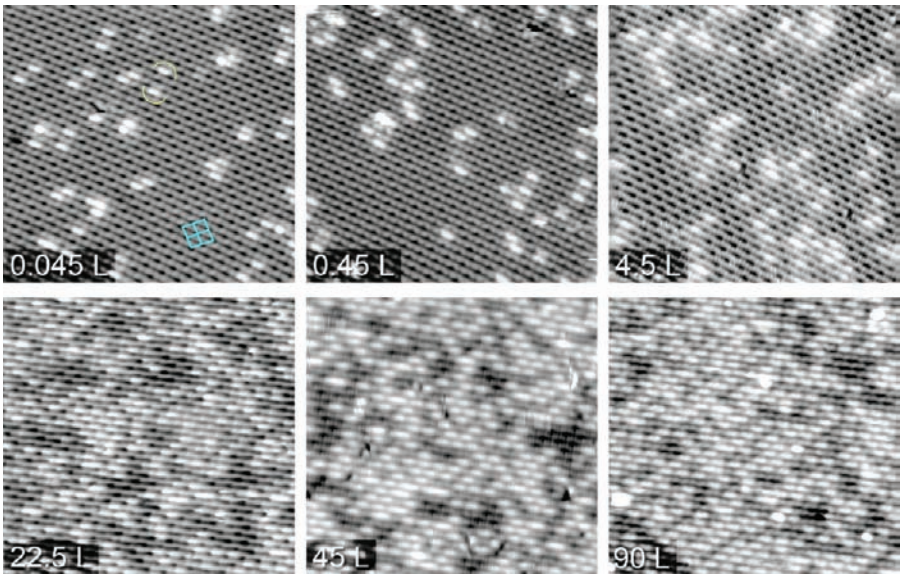

Figure 2. STM images (20×19 nm^2, V_{sample} = +0.9−1.2 V, I_{tunnel} = 0.28−0.34 nA) acquired after exposure of the clean $Fe_3O_4(001)$ surface to water with a nominal exposure as indicated. Four $(\sqrt{2} \times \sqrt{2})R45°$ unit cells are marked in the 0.045 L panel by cyan squares. Yellow half circles are used to indicate two O_SH species found in neighboring surface unit cells, which are paired as a result of dissociation of water at an oxygen vacancy.

of unit cells are now occupied and it is no longer possible to distinguish paired and isolated O_SH. For exposures greater than 45 L, the surface is almost saturated (0.0825 ML) with O_SH; again no other adsorbates are observed. Full saturation at one O_SH per unit cell equates to one atom per every eight surface O_S atoms (0.125 ML), apparently such a full coverage is never reached.

At saturation, the O_SH order with the same $(\sqrt{2} \times \sqrt{2})R45°$ periodicity of the underlying substrate, with a coverage of one O_SH per reconstructed surface unit cell. The LEED pattern observed for all water dosed surfaces demonstrated $(\sqrt{2} \times \sqrt{2})R45°$ periodicity, consistent with the ordered overlayer observed in STM. STM movies acquired at various coverages demonstrate H hopping over narrow sections between the Fe_S rows, again consistent with adsorption of H at the $O_{NAR.}$ sites.[20]

Figure 3 shows a plot of the average O_SH coverage in the STM images versus the nominal water dose in Langmuir. The offset of 0.01 ML is due to the O_SH pairs, which result from filling V_O's by dissociated water. Upon the onset of isolated O_SH adsorption, the coverage increases approximately linearly with exposure until saturation is observed at 0.0825 ML for exposures in excess of 45 L. The linear dependence of O_SH coverage on dose indicates that the dissociation of a single molecule is the rate-limiting step in the dissociation of water, at least for partial pressures up to 10^{-5} mbar. To check whether reactions between adsorbed H_2O could be necessary for dissociation, we performed experiments in which the total exposure was kept constant and the partial pressure and exposure time were varied. No discernible variation in the O_SH coverage was observed.

3.2. Low Energy Ion Scattering Studies. The most surprising observation from the STM investigations is the lack of evidence for O_WH species on the surface. Since STM probes the density of states of the surface and only indirectly the topography, it is possible that the O_WH may be present on the surface but not visible in the images. Moreover, if the O_WH species are mobile, it may also be difficult to observe them with STM at RT, although it should be pointed out that measurements on a cooled samples (T = 250 K) did not provide any evidence for O_WH either. Further cooling of

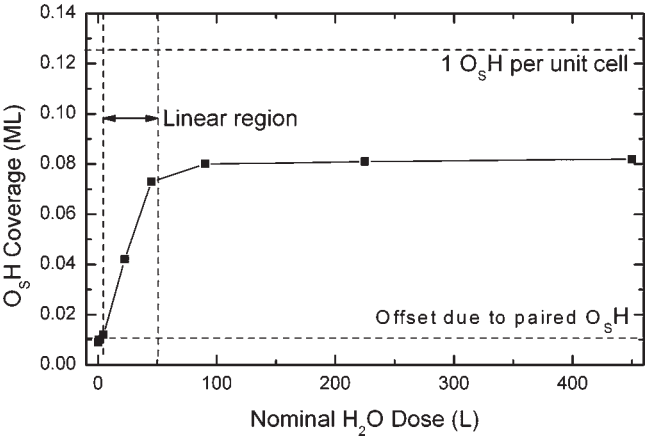

Figure 3. Plot of the average O_SH coverage observed in STM images versus the nominal water exposure in Langmuir.

the sample is complicated by the onset of molecular water adsorption around 230 K.[22] To further investigate whether the O_WH was present on the surface, we performed He^+ low energy ion scattering (LEIS) experiments using isotopically labeled $H_2{}^{18}O$ water. LEIS is a strictly surface sensitive technique and even small amounts of ^{18}O at the surface can be detected.[21] Figure 4a (top) shows LEIS spectra acquired from the clean $Fe_3O_4(001)$ surface and following saturation exposure (225 L) of $H_2{}^{18}O$. The data from these two surfaces are indistinguishable, with peaks due to elastic scattering from Fe and ^{16}O at 800 and 450 eV, respectively. An ^{18}O-related peak would be expected to appear at 495 eV, but is not observed.

In contrast, Figure 4b shows three LEIS scans acquired for the clean $Fe_3O_4(001)$ surface in a background pressure of $\sim 1 \times 10^{-8}$ mbar $H_2{}^{18}O$. The first scan resembles the data presented in Figure 4a, but during the third and fifth scans, an ^{18}O peak grows at the expense of the ^{16}O peak, up to a coverage of ~10% ML. We attribute this behavior to the reaction of the water with surface

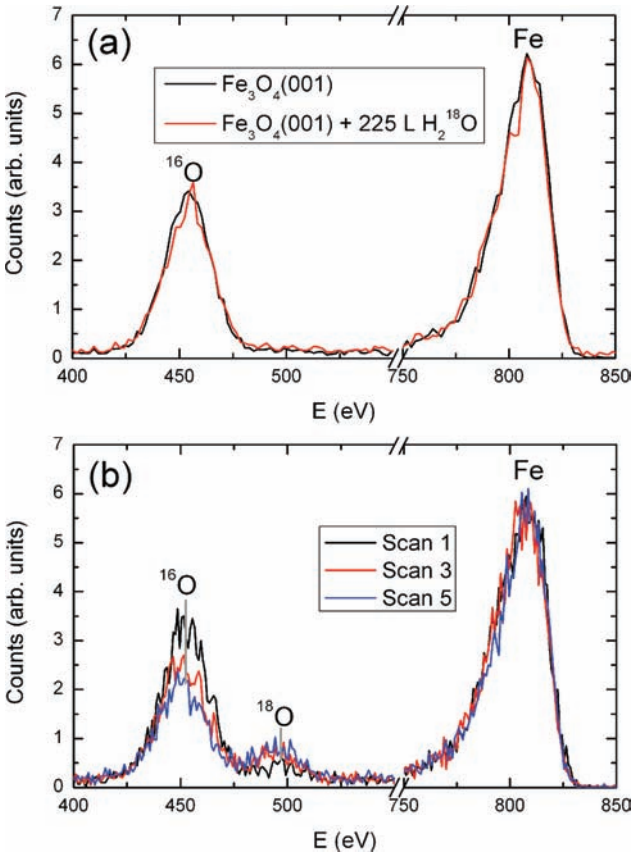

Figure 4. (a) LEIS data (1 keV He^+, scattering angle = 120°) acquired for the clean (black) and $H_2{}^{18}O$ saturated (red, 225 L $H_2{}^{18}O$ dose) Fe_3O_4(001) surface. No peak attributable to ^{18}O is observed. (b) LEIS data (1 keV He^+, scattering angle = 120°) acquired during repeated measurements of the clean Fe_3O_4(001) surface in an $H_2{}^{18}O$ background pressure of 1×10^{-8} mbar.

defects created during bombardment by the 1 keV He^+ ion beam.[21] Most importantly, however, the data presented in Figure 4b clearly demonstrate that the LEIS technique is sensitive to low concentrations of ^{18}O on the surface.

3.3. STM Studies: Desorption. Both the STM and LEIS studies of the water saturated Fe_3O_4(001) surface indicate that only hydrogenation of lattice oxygen occurs. However, in a prior temperature programmed desorption (TPD) study,[22] it was observed that molecular water desorption occurs at 520 K. To investigate the thermal desorption of the O_SH at the atomic scale, we flash-annealed the O_SH saturated surface (225 L) to various temperatures in the range of 373−873 K, before cooling the sample as quickly as possible back to room temperature for imaging with STM. Flash anneals up to 500 K do not significantly alter the appearance of the O_SH saturated surface. However, annealing to 520 K produces the image presented as Figure 5, which exhibits dark patches covering approximately 3.25% of the surface area. Mostly surrounding the dark patches we observe a small number of remnant O_SH species (~ 0.02 ML), while much of the surface resembles clean Fe_3O_4(001) (Figure 1b). Annealing at temperatures in excess of 550 K results in the disappearance of the dark patches and the recovery of the clean Fe_3O_4(001) surface.

From our experiments on the clean surface, we know that O vacancies appear as dark spots, and the dark patches are thus

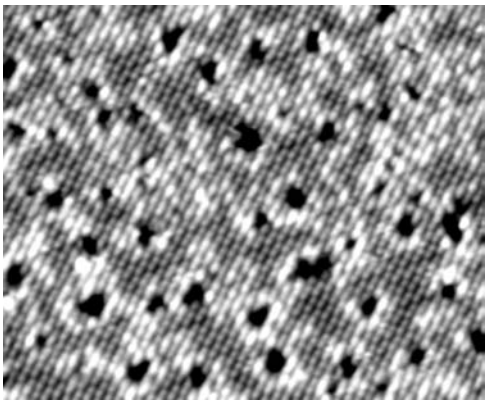

Figure 5. STM image (30×25 nm^2, V_{sample} = +0.94 V, I_{tunnel} = 0.3 nA) acquired following a flash anneal of the water saturated Fe_3O_4(001) surface (225 L) to 520 K. Dark areas linked to oxygen vacancies cover approximately 3.25% of the surface.

attributed to the loss of surface O when the water-exposed, H-covered surface is heated. To verify this, we performed two control experiments. First, the same annealing experiment was performed following adsorption of atomic H instead of water. This experiment resulted in similar dark patches to those shown in Figure 5. Second, the same annealing procedure was performed for the clean Fe_3O_4(001) surface, to no discernible effect.

4. DISCUSSION

The STM data presented in Figures 1 and 2 clearly demonstrate that dissociative water adsorption occurs on the stoichiometric Fe_3O_4(001) surface, in agreement with prior XPS experiments[23] and the predictions of DFT calculations.[24,25] The surprisingly low saturation coverage observed is linked to the limited availability of O_{NAR} sites, which are apparently necessary for the dissociation process. Remarkably, however, both the STM and isotopically labeled LEIS results indicate that O_WH is not present at the surface at room temperature, as would be expected on the basis of eq 2.

Further evidence for the missing O_WH comes from the dark patches observed upon thermal desorption of the O_SH (Figure 5). Ordinarily, heating an oxide surface with adsorbed dissociated water results in recombinative desorption of H and O_WH, and the surface returns to its original state. However, since no O_WH are present at the surface at room temperature, this process cannot occur. As a result, water desorption occurs at 520 K[22] through the abstraction of surface O_S atoms (Mars−van Krevelen mechanism, see eq 3), resulting in reduction of the surface and the appearance of the dark patches:

$$O_SH + O_SH \xrightarrow{\Delta} (H_2O)_g + O_S + V_O \quad (3)$$

Each desorbing water molecule removes 2 H atoms from the surface and creates one V_O. Twice the area covered by the V_O's (0.0325 ML in Figure 5) plus the remaining H coverage (0.02 ML) indeed sums to the original H coverage of 0.085 ML. Reduction of iron oxide surfaces has been shown to occur following exposure to CCl_4[26−28] and atomic H[29] as observed previously as well as confirmed in our own experiment. To our knowledge, this is the first example of an oxide surface being reduced following exposure to water. However, it should be

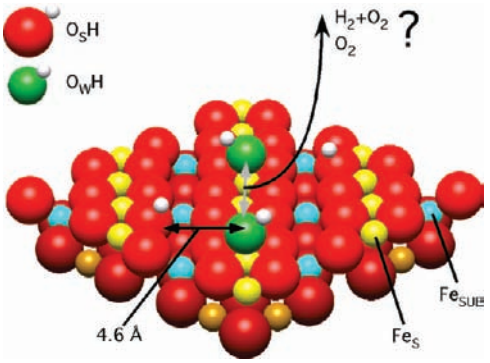

Figure 6. Schematic model showing the adsorption geometry predicted in recent DFT calculations[24,25] in which the O_SH and O_WH species are separated by 4.6 A. The O_WH species are situated on the Fe_S atoms (yellow). Facile diffusion along the Fe_S atom row (gray arrow) could lead to reactions between O_WH species, and subsequent desorption if the products are not bound to the surface at room temperature (e.g., H_2 and O_2, or O_2, leaving two adsorbed H atoms).

noted that the reduced surface is metastable and is reoxidized through O transfer from the bulk above 550 K. In addition, the surface can likely be reoxidized through reaction of water molecules with the oxygen vacancies, creating a hydroxylated surface consistent with eq 1.

Taken together, our results provide compelling evidence that only O_SH species are present at the surface following dissociative adsorption of water on the $Fe_3O_4(001)$ surface at room temperature. But where is the O_WH?

There are two possibilities; either O_WH diffuses into the crystal's bulk or it spontaneously desorbs in some form. Since the Fe_3O_4 lattice is composed of close-packed O^{2-} ions, diffusion should occur via place exchange, that is, hopping of V_O's. Our sample preparation procedure includes significant annealing in O_2, resulting in an extremely low V_O density (~0.005 ML at the surface). From our recent work[30] on the metastable Fe termination of $Fe_3O_4(001)$, where significant oxidation of the surface was not observed up to ~720 K, we conclude that mobility of O should be rather low at room temperature. Diffusion into the crystal's bulk is thus an unlikely explanation for the absence of O_WH. Moreover, if O_WH were to diffuse into the immediate subsurface region, we would expect to eventually uncover it during the LEIS measurements when the 1 keV He^+ beam sputters the surface. We performed extended LEIS measurements of the $H_2{}^{18}O$ saturated surface and no evidence for subsurface ^{18}O was observed.

Figure 6 shows a schematic model of the energetically favorable adsorption geometry for two dissociated water molecules (one molecule per surface unit cell) on the $Fe_3O_4(001)$ surface, as determined by recent DFT calculations.[24,25] The O_WH species are predicted to occupy sites atop the Fe_S row and the O_SH occupy O_{NAR} sites on the opposite sides of the unit cell. In this adsorption geometry, the separation between O_SH and O_WH on the surface is large (4.6 Å), which likely represents a significant barrier to recombination. Furthermore, the O_SH forms an H bond to the neighboring O_{NAR} atom,[20] further strengthening its bond to the surface. Since recombinative desorption does not occur at room temperature, we can estimate that the resulting barrier to recombination is at least 18.1 kcal/mol.[31] Consequently, an alternative process must lead to desorption of O_WH from the surface. From our experiments, we cannot rule out that the O_WH radical simply leaves the surface, but we are not aware of any precedent for OH radical desorption from a surface in the absence of photons or other ionizing radiation.[32,33] Alternatively, two O_WH may come together to react together forming a third species that is not bound to the surface at room temperature. While Figure 6 demonstrates how the $H-O_WH$ reaction may be suppressed by the adsorption geometry, facile diffusion of the O_WH species along the Fe_S rows could facilitate O_WH-O_WH reactions and a significant reaction rate realized through an increase in the preexponential factor, that is, frequent attempts at a reaction.

The reaction of two O_WH could conceivably result in H_2 plus O_2, O_2 plus two adsorbed O_SH, H_2O plus an adsorbed O, or possibly formation of H_2O_2. However, we can rule out H_2O and one adsorbed O atom since we do not observe any ^{18}O in either LEIS or STM. Moreover, we consider production of H_2O_2 to be unlikely since it is a less energetically favorable product than H_2 and O_2. As mentioned above, we have found that neither O_2 nor H_2 sticks to the $Fe_3O_4(001)$ surface at room temperature, which suggests that both species would desorb immediately upon formation in the current experiments. However, as the expected amounts are small (total of <0.04 ML over an extended time period in a high water background), they cannot be detected with our experimental setup. Irrespective of the actual reaction products, however, our results suggest that water is split upon reaction with the $Fe_3O_4(001)$ surface at room temperature.

5. CONCLUSIONS

In summary, we describe a hitherto unreported adsorption behavior for water, in which dissociative adsorption at room temperature results only in the hydrogenation of the oxygen lattice. Heating of the hydrogenated surface leads to extraction of lattice oxygen atoms to form water; thus, water exposure leads to the *reduction* of $Fe_3O_4(001)$ under UHV conditions. We attribute this surprising behavior to reactive desorption of O_WH species at room temperature, effectively splitting water at room temperature. This unusual reaction process may occur because the energetically favorable adsorption geometry for dissociated water on $Fe_3O_4(001)$ kinetically hinders recombinative desorption, but facilities O_WH-O_WH interactions.

AUTHOR INFORMATION

Corresponding Authors

parkinson@iap.tuwien.ac.at; diebold@iap.tuwien.ac.at

ACKNOWLEDGMENT

This material is based upon work supported as part of the Center for Atomic-Level Catalyst Design, an Energy Frontier Research Center funded by the U.S. Department of Energy, Office of Science, Office of Basic Energy Sciences under Award Number #DE-SC0001058. The authors acknowledge Prof. Mao (Tulane University) for the synthetic sample used in this work and discussions with Narasimham Mulakaluri, Dr. Rossitza Pentcheva (Univ. Munich), Prof. Dr. Matthias Scheffler (Fritz-Haber Institute, Berlin), and Prof. Phillip Sprunger (Louisiana State University).

REFERENCES

(1) Thiel, P. A.; Madey, T. E. *Surf. Sci. Rep.* **1987**, *7*, 211.
(2) Henderson, M. A. *Surf. Sci. Rep.* **2002**, *46*, 5.

(3) Michaelides, A. *Appl. Phys. A: Mater. Sci. Process.* **2006**, *85*, 415.
(4) Verdaguer, A.; Sacha, G. M.; Bluhm, H.; Salmeron, M. *Chem. Rev.* **2006**, *106*, 1478.
(5) Hodgson, A.; Haq, S. *Surf. Sci. Rep.* **2009**, *64*, 381.
(6) Diebold, U. *Surf. Sci. Rep.* **2003**, *48*, 53.
(7) Diebold, U.; Li, S. C.; Schmid, M. *Annu. Rev. Phys. Chem.* **2010**, *61*, 129.
(8) Sun, C. H.; Liu, L. M.; Selloni, A.; Lu, G. Q.; Smith, S. C. *J. Mater. Chem.* **2010**, *20*, 10319.
(9) Calzolari, A.; Catellani, A. *J. Phys. Chem. C* **2009**, *113*, 2896.
(10) Kunat, M.; Girol, S. G.; Burghaus, U.; Woll, C. *J. Phys. Chem. B* **2003**, *107*, 14350.
(11) Onsten, A.; Stoltz, D.; Palmgren, P.; Yu, S.; Gothelid, M.; Karlsson, U. O. *J. Phys. Chem. C* **2010**, *114*, 11157.
(12) Wander, A.; Harrison, N. M. *J. Chem. Phys.* **2001**, *115*, 2312.
(13) Dulub, O.; Meyer, B.; Diebold, U. *Phys. Rev. Lett.* **2005**, 95.
(14) Meyer, B.; Marx, D.; Dulub, O.; Diebold, U.; Kunat, M.; Langenberg, D.; Woll, C. *Angew. Chem., Int. Ed.* **2004**, *43*, 6642.
(15) Pentcheva, R.; Wendler, F.; Meyerheim, H. L.; Moritz, W.; Jedrecy, N.; Scheffler, M. *Phys. Rev. Lett.* **2005**, *94*, 126101.
(16) Pentcheva, R.; Moritz, W.; Rundgren, J.; Frank, S.; Schrupp, D.; Scheffler, M. *Surf. Sci.* **2008**, *602*, 1299.
(17) Tarrach, G.; Burgler, D.; Schaub, T.; Wiesendanger, R.; Guntherodt, H. J. *Surf. Sci.* **1993**, *285*, 1.
(18) Stanka, B.; Hebenstreit, W.; Diebold, U.; Chambers, S. A. *Surf. Sci.* **2000**, *448*, 49.
(19) Ceballos, S. F.; Mariotto, G.; Jordan, K.; Murphy, S.; Seoighe, C.; Shvets, I. V. *Surf. Sci.* **2004**, *548*, 106.
(20) Parkinson, G. S.; Mulakaluri, N.; Losovyj, Y.; Jacobson, P.; Pentcheva, R.; Diebold, U. *Phys. Rev. B* **2010**, *82*, 125413.
(21) Pan, J. M.; Maschhoff, B. L.; Diebold, U.; Madey, T. E. *J. Vac. Sci. Technol., A* **1992**, *10*, 2470.
(22) Peden, C. H. F.; Herman, G. S.; Ismagilov, I. Z.; Kay, B. D.; Henderson, M. A.; Kim, Y. J.; Chambers, S. A. *Catal. Today* **1999**, *51*, 513.
(23) Kendelewicz, T.; Liu, P.; Doyle, C. S.; Brown, G. E.; Nelson, E. J.; Chambers, S. A. *Surf. Sci.* **2000**, *453*, 32.
(24) Mulakaluri, N.; Pentcheva, R.; Scheffler, M. *J. Phys. Chem. C* **2010**, *114*, 11148.
(25) Mulakaluri, N.; Pentcheva, R.; Wieland, M.; Moritz, W.; Scheffler, M. *Phys. Rev. Lett.* **2009**, *103*, 176102.
(26) Rim, K. T.; Muller, T.; Fitts, J. P.; Adib, K.; Camillone, N.; Osgood, R. M.; Batista, E. R.; Friesner, R. A.; Joyce, S. A.; Flynn, G. W. *J. Phys. Chem. B* **2004**, *108*, 16753.
(27) Adib, K.; Camillone, N.; Fitts, J. P.; Rim, K. T.; Flynn, G. W.; Joyce, S. A.; Osgood, R. M. *Surf. Sci.* **2002**, *497*, 127.
(28) Parkinson, G. S.; Dohnalek, Z.; Smith, R. S.; Kay, B. D. *J. Phys. Chem. C* **2009**, *113*, 1818.
(29) Huang, W. X.; Ranke, W. *Surf. Sci.* **2006**, *600*, 793.
(30) Parkinson, G. S.; Novotny, Z.; Jacobson, P.; Schmid, M.; Diebold, U. *Surf. Sci. Lett.* **2011**, *605*, L42.
(31) Value calculated using Arrheneus kinetics assuming a low reaction rate (0.1/s), a preexponential factor of 10^{13}/s, and a temperature of 292 K.
(32) Thiebaud, J.; Thevenet, F.; Fittschen, C. *J. Phys. Chem. C* **2010**, *114*, 3082.
(33) Vincent, G.; Aluculesei, A.; Parker, A.; Fittschen, C.; Zahraa, O.; Marquaire, P. M. *J. Phys. Chem. C* **2008**, *112*, 9115.